THE JOURNAL OF PHYSICAL CHEMISTRY C

Article

pubs.acs.org/JPCC

Optimally Designed Nanoshell and Matryoshka-Nanoshell as a Plasmonic-Enhanced Fluorescence Probe

Tianyue Zhang,[†] Guowei Lu,*[,†] Wenqiang Li,[†] Jie Liu,[†] Lei Hou,[†] Pascal Perriat,[‡] Matteo Martini,[§] Olivier Tillement,[§] and Qihuang Gong*[,†]

[†]State Key Laboratory for Mesoscopic Physics, Department of Physics, Peking University, Beijing 100871, China

[‡]MATEIS, UMR 5510 CNRS, INSA-Lyon, Université de Lyon, 20 av. Albert Einstein, 69621 Villeurbanne Cedex, France

[§]LPCML, Université de Lyon, Université Claude Bernard, 43 Bd du 11 novembre 1918, 69622 Villeurbanne Cedex, France

Supporting Information

ABSTRACT: Nanoshell and Matryoshka-nanoshell constructs are rationally optimized utilizing the finite-difference time-domain method to design probes with enhanced fluorescence. Through the systematical investigation of interactions between the spontaneous emission of a single emitter and a metal-based nanostructure, the plasmonic-enhanced fluorescence is found maximal for certain morphologies that balance two competitive factors: field enhancement and quantum efficiency. For instance, key parameters such as the emitter's position, its orientation, and the spectral overlaps between molecular bands and plasmon resonance are investigated to fully understand the complete behavior of the system. In the case of metal nanoshells, it is shown that the molecular fluorescence is differently enhanced inside or outside the shell. In that of Matryoshka-nanoshells that consist of concentric gold core and shell, the construct appears as an exceptionally promising probe especially when the fluorophore lies within the gap layer. Indeed, the strong coupling between the adjacent core and shell allows electromagnetic excitation to be squeezed within the gap, so resulting in giant fluorescence and photostability. Such a construct opens a way for still increasing the sensitivity of fluorescence detection, which is promising for almost all biological imaging applications.

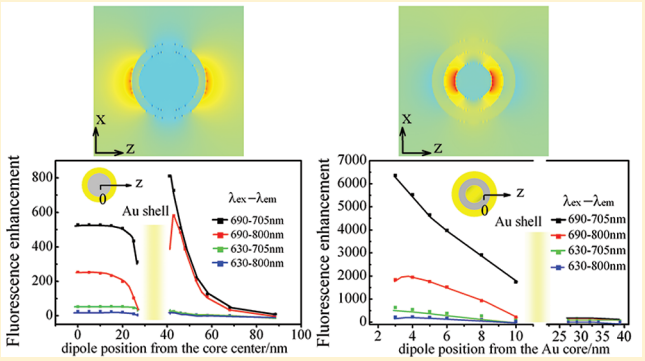

INTRODUCTION

Fluorescence imaging is a powerful technique increasingly used in current biochemical research, such as disease diagnosis, genomic analysis, and proteomic studies.[1−3] This rapidly progressing technique requires fluorescent probes with always higher photostability and emission intensity to push forward the sensitivity of fluorescence detection. The list of fluorescence probes continues to grow from organic dyes to quantum dots and biocompatible low cytotoxicity nanoparticles.[4−8] Further emerging developments are aiming to achieve high-resolution and lifetime-based fluorescence imaging.[9,10] Noble metallic nanoparticles exhibit extraordinary surface plasmon resonances that interact strongly with optical fields known as optical antennas. A near-field interaction is observed to occur when fluorophores are placed in the vicinity of a metallic nanoparticle, which result in significant improvement of fluorescent performances. Among various types of metal nanoparticles, metallic nanoshell (NS) comprising a dielectric core (silica) surrounded by a thin metallic shell (gold or silver) is a particularly attractive one, which can be designed systematically with plasmon resonances from the visible to infrared regions of the spectrum by varying the relative dimensions of the core and shell thickness.[11,12] To date, nanoshells have shown their potentials in applications ranging from tunable plasmonic substrates for Raman enhancement,[13] to light-triggered drug delivery and release,[14] to immunoassay diagnosis,[15] and to hybridization with the target molecules for cell imaging.[16,17] Metallic nanoshells are especially suitable as NIR fluorescence probes because their plasmon resonance wavelength easily spans the near-infrared region where biological tissues display minimal autofluorescence and absorption.

Numerous experimental and theoretical studies have been reported on the fluorescence behaviors of molecules at the vicinity of nanoshells lying on the outside surface or encapsulated within the nanoshell. For instance, Halas et al. observed remarkable fluorescence intensity and decay rates enhancement for fluorophores conjugated to a nanoshell outside surface when the plasmon resonance corresponds to the emission frequency of the molecules.[18,19] In contrast, encapsulation of molecules inside nanoshell cavities has also attracted considerable attention, leading to increases in fluorescence brightness, shortened fluorescence lifetime, and

Received: December 30, 2011
Revised: February 27, 2012
Published: March 21, 2012

extended photostability.[20−24] Nanoconstructs made of gold nanoshells acting as transparent plasmonic nanocontainers permitted one to greatly improve the photoresistance of encapsulated organic dyes.[25] To simulate the plasmonic effects upon fluorescence, theoretical studies use both analytical and numerical methods. For instance, it was demonstrated that, in the cavity of a Ag nanoshell, the molecular fluorescence was significantly enhanced, whereas the fluorescence lifetime was dramatically decreased.[26,27] Miao et al. calculated the field distribution around a gold nanoshell and optimized a core−shell structure to maximize the light absorption of an emitter.[28] Also, the Purcell effect caused by a nanoshell dimer upon the fluorescence of a single molecule placed within the gap was theoretically studied.[29]

However, even if previous reports have addressed some of the fundamental phenomena that explain the interactions between metallic nanoshells and nearby molecules, a systematic understanding of the complete molecular fluorescence behaviors near (both outside and within) a nanoshell is still lacking. In particular, the optimal structure of the nanoshell required to achieve a highly efficient fluorescence enhancement is still unrevealed. The main objective of this study is then to define the optimal design of such nanoshells by systematic calculation of key parameters such as the molecule−nanoshell separation, the molecule orientation, or the incident light polarization. By an extensive use of the finite-difference time-domain (FDTD) method, we demonstrated that the more efficient morphology of the nanoconstruct was the so-called Matryoshka-nanoshell (MNS). This nanoconstruct consists of two concentric metal core and corona so delimitating a cavity filled with a dielectric layer in which fluorophores can be encapsulated. Such multishell construct for designing and controlling surface enhanced Raman scattering[30] and tuning plasmon related scattering or absorption has received much attention.[31] Yet the potential of such nanoconstruct for modulating molecular spontaneous emission has been surprisingly underappreciated. The geometry is very efficient for fluorescence enhancement because the excitation field is increased within the cavity, whereas the fluorophore quantum yield undergoes only minor alterations. Moreover, such MNS configurations are experimentally feasible, for instance, by a microemulsion method in which the reactive reagents are successively added in a nanoreactor. In this Article, the parameters of the MNSs are optimized to obtain maximal plasmonic-enhanced fluorescence, which permits one to define promising probes in the field of fluorescence imaging and detection.

METHODS

FDTD method is a powerful technique used for simulating both near- and far-field electromagnetic responses of metal nanostructures with arbitrary geometries.[32,33] This method has been extensively tested and applied for calculating decay rates near a metallic nanostructure, electromagnetic field distribution, and absorption and scattering cross sections of various nanostructures. To fully understand the interactions between a metallic nanostructure and a fluorophore, a configuration comprising a single emitter and a single metal structure needs to be studied. We then consider an isolated emitter with a radiative decay rate Γ^0_{rad}, a nonradiative decay rate Γ^0_{nrad}, and a quantum efficiency $\eta_0 = \Gamma^0_{rad}/(\Gamma^0_{rad} + \Gamma^0_{nrad})$. All of these parameters depend on the frequency ω. The presence of a metallic NS introduces an additional nonradiative decay channel due to absorption in the metal. It modifies also the radiative decay rate now denoted Γ_{rad} that accounts for the energy reaching the far field. When the isolated emitter is coupled to the nanoantenna, its quantum efficiency changes to:

$$\eta_{(\omega)} = \eta_{0(\omega)}/[(1 - \eta_{0(\omega)})/F_{(\omega)} + \eta_{0(\omega)}/\eta_{a(\omega)}] \quad (1)$$

In this relation, $F(\omega) = \Gamma_{rad}/\Gamma^0_{rad}$ is the Purcell factor, representing the enhancement of the radiative decay rate, and $\eta_a(\omega) = \Gamma_{rad}/(\Gamma_{rad} + \Gamma_{nrad})$ is the antenna efficiency, which is the power that reached the far field divided by the total emitting power. When the metal and the emitter interact in a way that the dipolar radiation pattern of the isolated emitter is almost not perturbed, the field intensity enhancement and Purcell factor are related. Given this condition, the fluorescence enhancement S/S_0 can be well approximated by replacing the electric field enhancement where p is the transition electric dipole moment $|pE|^2/|pE_0|^2$ by the Purcell factor F.[34−36] The fluorescence enhancement becomes:

$$\frac{S}{S_0} = \frac{\eta_{(\omega)}|pE|^2}{\eta_{0(\omega)}|pE_0|^2} \approx F_{(\omega)}\frac{\eta_{(\omega)}}{\eta_{0(\omega)}} \quad (2)$$

From the above equations, the fluorescence enhancement depends now on the Purcell factor $F(\omega)$ and on the antenna efficiency $\eta_a(\omega)$, with the initial quantum efficiency $\eta_0(\omega)$ serving as a reference for evaluating the enhancement. As was said in the Introduction, we focus our attention on NS consisting of silica core/gold shells and on MNS based on the same materials, that is, gold core/silica layer/gold shell. The optical dielectric function of gold is modeled using the Drude−Lorentz dispersion model,[37] and the refractive index of the different media was considered independent of frequency and was equal to 1.33 for water and 1.49 for silica. The FDTD mesh discretization is chosen to be 0.5 nm with termination of the FDTD mesh by perfectly matched-layers (PML) characterized by absorbing boundary conditions.

RESULTS AND DISCUSSION

Optimization of a NS−Emitter Configuration for High Fluorescence Enhancement. The plasmon resonances of a NS are usually explained as the interaction or hybridization of the sphere and cavity plasmons.[31,38] Theoretical work has revealed that, when decreasing the shell thickness, there is a near-exponential red-shift in the wavelength maximum of the plasmon resonance, and that this shift is also dependent on the NS size.[39] Our calculation results completely coincide with the above conclusions: in particular, the resonance of the gold nanoshell plasmon can be tuned through adjusting both the silica core radius and the gold shell thickness (see the Supporting Information). In practice, it is desirable to design and fabricate the best fluorescent probe adapted to the chosen fluorophore dye. Here, Rhodamine 800 (Rh800) was selected as the representative molecule of the study because this near-infrared-emitting dye is extensively used in clinical biomedical researches such as fluorescence microscopy, flow cytometry, and ELISA.[40−42] Rh800 is a remarkably weak fluorophore with a quantum yield below 10% with absorption and emission wavelengths lying at 680 and 705 nm, respectively.[40] Next, the easily tunable plasmon resonance of gold NSs allows us to choose favorable parameters (size or core/shell-ratio), permitting a plasmon correspondence with the absorption or emission

dx.doi.org/10.1021/jp2125944 | J. Phys. Chem. C 2012, 116, 8804−8812

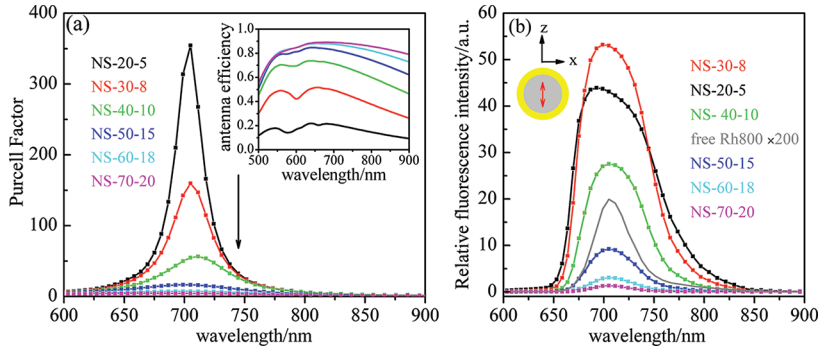

Figure 1. Normalized Purcell factor F (a) and antenna efficiency η_a (inset) for different nanoshells (in the figure are indicated successively the silica core radius and the gold shell thickness) having a plasmon resonance at 705 nm. Relative fluorescence intensity (b) of a single Rh800 molecule placed in the center of nanoshells for excitation at a wavelength of ~690 nm, and the relative fluorescence intensity of free Rh800 molecule is plotted in gray for comparison. The molecules are polarized along the z direction.

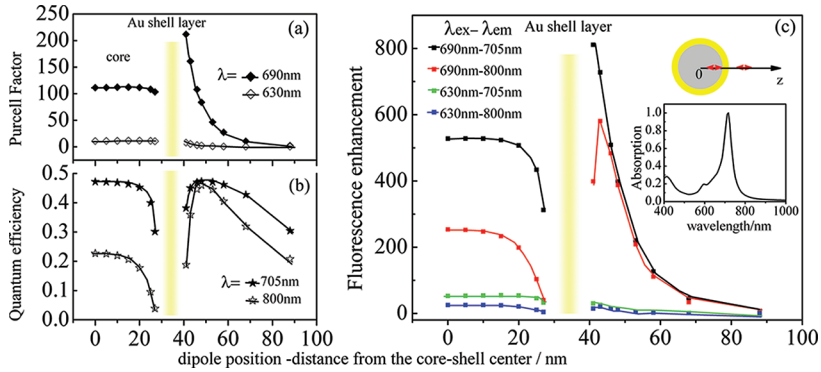

Figure 2. Purcell factor (a, top left), normalized quantum efficiency (b, bottom left), and fluorescence enhancement (c) for an emitter coupled to a "NS-30-8" (silica core radius = 30 nm, gold shell thickness = 8 nm) as a function of the emitter-nanoshell position (inside or outside the nanoshell) at different excitation and emission wavelengths. The inset in (c) shows the absorption spectrum of the "NS-30-8". The emitter is polarized along the z axis.

maxima of the fluorophore to achieve expected fluorescence enhancements.

Previous studies of spherical nanoparticle were reported to quench or enhance the fluorescence,[43−47] the spontaneous emission of single molecule depending on metal distance.[44,48] The fluorescence quenching that happens when the emitter−particle separation is very small can be reduced by designs of the metal morphology such as nanorods or ellipsoids for which the radiative decay rates overshadow the nonradiative loss near plasmon resonance.[35,36,49,50] Another condition permitting to reduce the quenching near metal and even leading to remarkable fluorescence enhancement consists of adjusting the plasmon resonance to the maximum of the emission frequency of the molecules.[18] In this Article, we will begin by showing that NS constructs are also able to enhance any fluorophore spontaneous emission for very short separations theoretically defined by plasmonic engineering based upon FDTD calculations.

To reduce the fluorescence quenching at short emitter−particle separation, NSs with different core radii are chosen, and their dipolar plasmon resonances are all tuned nearly 705 nm (a value corresponding to the emission peak of Rh800) by a simple adjustment of their shell thickness. Figure 1a shows the Purcell factor F and the antenna efficiency η_a for the different NSs investigated. It can be found that, in the whole wavelength range, the Purcell factor F increases while the antenna efficiency η_a decreases with reducing the NS's dimension. To enhance efficiently the fluorescence, the system is required to have a strong local enhanced optical field and at the same time a large Purcell factor F and a high antenna efficiency η_a. These conditions cannot be satisfied simultaneously for a single plasmonic nanoparticle as shown in Figure 1. For instance, large spherical particles usually present high scattering cross section over the absorption one, which results in a higher antenna efficiency as compared to those with a smaller size. Unfortunately, high antenna efficiency usually means a faster radiative damping rate, which reduces both the quality factor and the field enhancement.[44,48,51] Our simulation results shown in Figure 1a prove all of these features, in particular, that a high antenna efficiency also corresponds to a low Purcell factor for the geometry of a NS. They also emphasize the fact that calculations are indispensable to determine the optimal characteristics of NS structures because an optimized fluorescence enhancement needs to realize a balance between a lot of geometrical parameters.

Given that the initial quantum efficiency η_0 is 0.1 at $\lambda \approx 705$ nm, we calculate the relative fluorescence intensity of Rh800 excited by an excitation wavelength at 690 nm (Figure 1b). Among the NSs studied in Figure 1a, the "NS-30-8" (denoting a NS with a 30 nm core radius and an 8 nm-thick shell) is the one that presents the highest enhancement effect upon a single fluorescent molecule being placed at its center. This NS presents then the best compromise between two features varying in opposite directions, the Purcell factor F and the antenna efficiency η_a. Note that the fluorescence enhancement was also calculated in the cases where the emitters were placed

dx.doi.org/10.1021/jp2125944 | J. Phys. Chem. C 2012, 116, 8804−8812

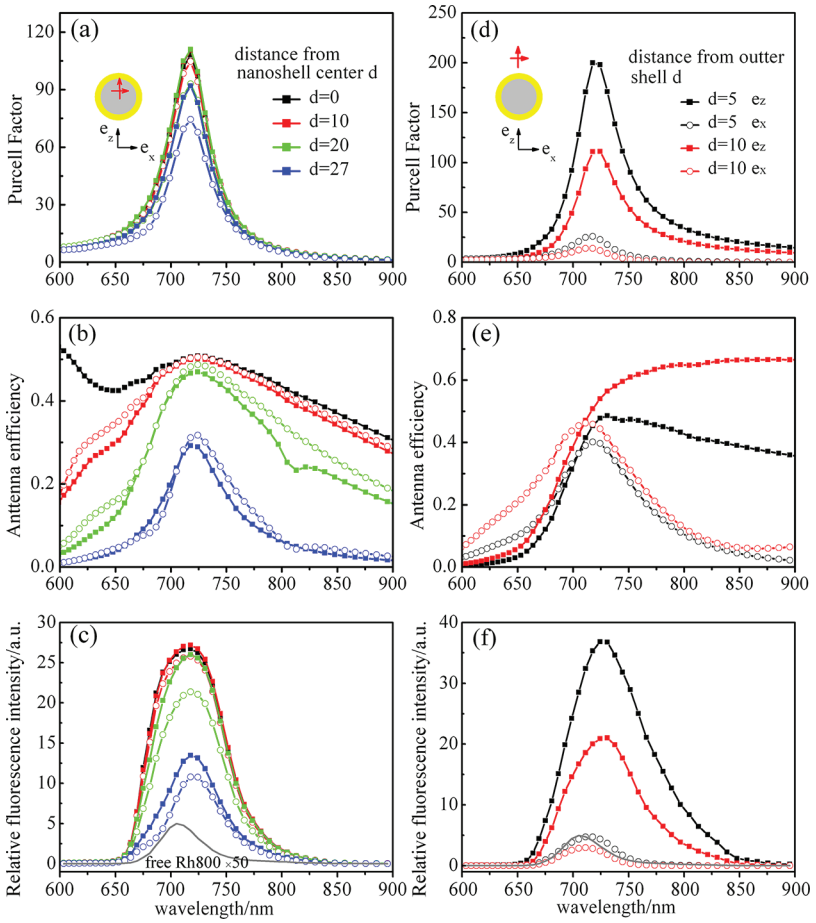

Figure 3. Purcell factor, antenna efficiency, and relative fluorescence intensity. The emitter is placed inside (left) or outside (right) the "NS-30-8". The footnote square and circle represent the orientation of the dipole with e_z and e_x. The separation between the emitter and the center of the nanoshell is fixed at 0, 10, 20, and 27 nm when the emitter is placed inside the NS. The separation between the emitter and the nanoshell outer surface is fixed at 5 and 10 nm when the emitter is placed outside. The relative fluorescence intensity of free Rh800 molecule is plotted in gray for comparison.

at the exterior of the NS and also lead to the same result that the "NS-30-8" gave the best fluorescence enhancement (data not shown). It is worthy that the optimization of the parameters of the NSs for other dye molecules is quite similar and only different in overall sizes and core−shell ratios. To change the parameters, it is sufficient to reach the new plasmon resonance by using the above-mentioned near-exponential decay of the resonance wavelength that depends on both the shell thickness and the core radii.[39]

After having demonstrated the NS size effects upon fluorescence enhancement, we now examine the relative position of the emitter, respectively, to the NS because this latter could also significantly influence the fluorescence behaviors. Figure 2 displays the Purcell factor F, the quantum efficiency η, and the fluorescence enhancement as functions of the separation between the emitter and the NS center (in other words, an emitter polarized along the z direction is placed at various positions on the radial axis of the "NS-30-8" that was previously recognized as the NS leading to the greatest enhancement). Within the core region, the Purcell factor and the quantum efficiency experiments show only small variations except at positions very close to the internal gold surface of the NS, so that the fluorescence enhancement presents a similar behavior (Figure 2). When the emitter is placed outside the NS, the Purcell factor at $\lambda \approx 690$ nm significantly increases at the very vicinity of the outer shell surface. This is related to the field distribution around the NS, the optical intensity within the core region being much more uniform than at the NS outside as will be shown later. Concerning the quantum efficiency, the latter strongly declines the fluorescence enhancement near both internal and external shell surfaces due to the strong nonradiative loss of the metal.

Finally, the maximum of fluorescence enhancement is achieved when the plasmon resonance of the NS overlaps both the excitation and the emission spectra of the emitter as shown in Figure 2c (i.e., when excitation and emission are at $\lambda \approx 690$ and 705 nm, respectively). Indeed, when excitation deviates from the plasmon resonance, a lower excitation rate and a smaller field enhancement are obtained, resulting in a weaker fluorescence enhancement. Also, when the plasmon resonance deviates from the peak of molecular emission, this leads to a lower quantum efficiency correlated to fluorescence quenching at immediate proximity of the surface. However, the calculations made unexpectedly demonstrate that the plasmonic enhancement of fluorescence does not depend only on the distance and on the wavelength but also on the curvature of the metal shell because the fluorescence enhancement gives rise to different trends in the internal and external regions of the NS (Figure 2c). When an emitter is placed outside the NS (convex region), even very close to the metal surface, the molecular

dx.doi.org/10.1021/jp2125944 | J. Phys. Chem. C 2012, 116, 8804−8812

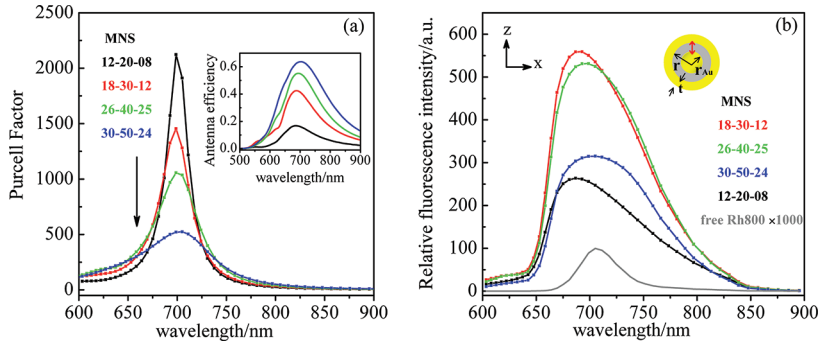

Figure 4. Normalized Purcell factor F (a) and antenna efficiency η_a (inset) for different Matryoshka-nanoshells (denoted in the figure as the form of radius of gold core−radius of silica layer−gold shell thickness) with the plasmon resonance located at 705 nm, and the relative fluorescence intensity of a single Rh800 molecule inside the nanoshells 4 nm from the gold core surface for excitation at the wavelength ~690 nm, and free Rh800 molecule is plotted in gray for comparison (b).

fluorescence can be remarkably enhanced if the plasmon resonance of the NS is designed to correspond with the emission band of the fluorophore. As seen in Figure 2c, a high fluorescence enhancement is observed for emitter−metal separation as small as 3 nm, which means that the quenching is not yet dominating at distances normally smaller than the Förster one.[44,46−49] Thus, if one aims at detecting the fluorescence of a single molecule, the best solution consists of bonding the molecule outside the NS because this geometry will give more fluorescence intensity provided nevertheless that both NS plasmonic resonance and molecule position are precisely adjusted. However, even if within the NS (concave region), the fluorescence near the metallic shell always presents an important quenching effect regardless of the wavelength used, and it remains still possible to encapsulate a large number of fluorescent molecules within the NS to obtain a significant fluorescence signal. These conclusions should be moderated by the fact that the present simulation is based on single dipole calculations and then does not take into account the interactions between the molecules that can be responsible of phenomena such as fluorescence quenching due to concentration.[21] However, this latter phenomenon, which is beyond the scope of this study, has been recently shown to be almost suppressed by the presence of metal plasmon.[52]

All of the above calculations were performed for an emitter orientated along the z direction and moved on the radial axis in cylindrical coordinates. To deeper investigate the effects of the polarization of an emitter−nanoshell system, 3D-FDTD calculations have to be performed. A dipole is then placed at various positions with different orientations to the "NS-30-8". Because of the NS's symmetry, two orientations denoted as e_z and e_x have to be considered (precisely e_z refers to the radial axis, whereas e_x refers to the axis perpendicular to the radial one). The fluorescence enhancement is calculated through a two-stage process, that is, by separate calculations of the excitation field enhancement and the emission quantum efficiency.[34] Typical results are shown in Figure 3, the orientation dependence of the fluorescence within the NS core region presenting distinct behaviors as compared to regions outside the NS.

The trends shown by the position evolution of F, η_a, and fluorescence enhancement when these latter are evaluated by 3D-FDTD calculations are consistent with those results obtained using 2D calculations. The left column in Figure 3 concerns the emitters that are placed within the NS core region. Those with polarization along e_z present Purcell factor and antenna efficiency similar to those polarized along e_x. This is consistent with the characteristics of the optical field distribution around the metal NS that presents only slight differences under illumination polarized according to the e_x or e_z directions. The fluorescent emitters embedded within the NS then can experience substantial fluorescence enhancement whatever the location of the molecules and their dipolar orientation. However, for the emitter located outside the NS, there is a strong molecular orientation dependence of the plasmonic-enhanced fluorescence as shown in the right panel of Figure 3. Indeed, the emitter oriented along e_z presents a significantly greater enhancement than that related to the emitter oriented along e_x placed at the same position. Because the coupling between the emitter and the NS is more efficient for dipoles along e_z, both molecular orientation and excitation polarization should be taken into account during optimization of the NS−emitter fluorescent system.

Optimization of a Matryoshka-Nanoshell (MNS) for High Fluorescence Enhancement. After having demonstrated several key parameters affecting the spontaneous emission behaviors near NSs, the following question arises naturally: Is NS the best structure to enhance the fluorescence of an emitter with more efficiency? Given that pairs of adjacent metallic nanoparticles give rise to enormous field enhancement within the gap because of a giant plasmonic coupling effect, other constructs using this property could be easily imagined. This configuration permits the formation of an electromagnetic "hot spot" useful for single molecule detection in the famous surface enhanced Raman scattering (SERS) technique.[53] Similarly, multilayered core−shells present a strong plasmonic coupling and hybridizing between the core and all of the metallic shells.[31,54] These multilayered constructs (called Matryoshka-nanoshells (MNS)) are known to lead to extremely large field enhancements[30,54] and, more generally, to interesting plasmon Fano resonance phenomena involving plasmonics.[55] Matryoshka-nanoshells (MNSs) with a metal core and alternating dielectric and metal shells can act as a collection of optical condensers that focus the light toward the cavity lying between the core and the innermost metal shell. These constructs that have already been designed for SERS[30] are tested here for improving plasmonic-based fluorescence enhancement. Given this objective, the optimization of MNSs as fluorescence probes will be made with special care for distinguishing the relative contributions of quantum efficiency, antenna efficiency, decay rates, and field enhancements.

dx.doi.org/10.1021/jp2125944 | J. Phys. Chem. C 2012, 116, 8804−8812

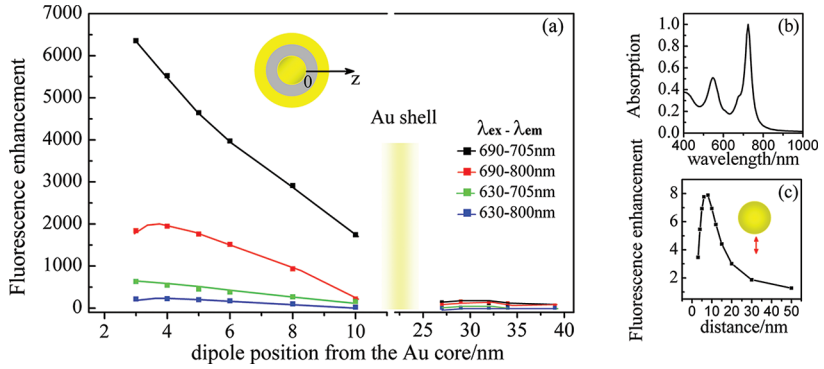

Figure 5. Fluorescence enhancement (a) for an emitter coupled to "MNS-18-30-12" (gold core radius = 18 nm, silica layer thickness = 12 nm, and gold shell thickness = 12 nm) as a function of the emitter−nanoshell position (inside and outside the nanoshell) at different excitation and emission wavelengths. The absorption spectrum of the "MNS-18-30-12" is shown in (b). Fluorescence enhancement for an emitter coupled to an Au nanosphere with radius 18 nm is plotted in (c) as a function of the emitter−particle separation with excitation by ∼690 nm light and emission at 705 nm.

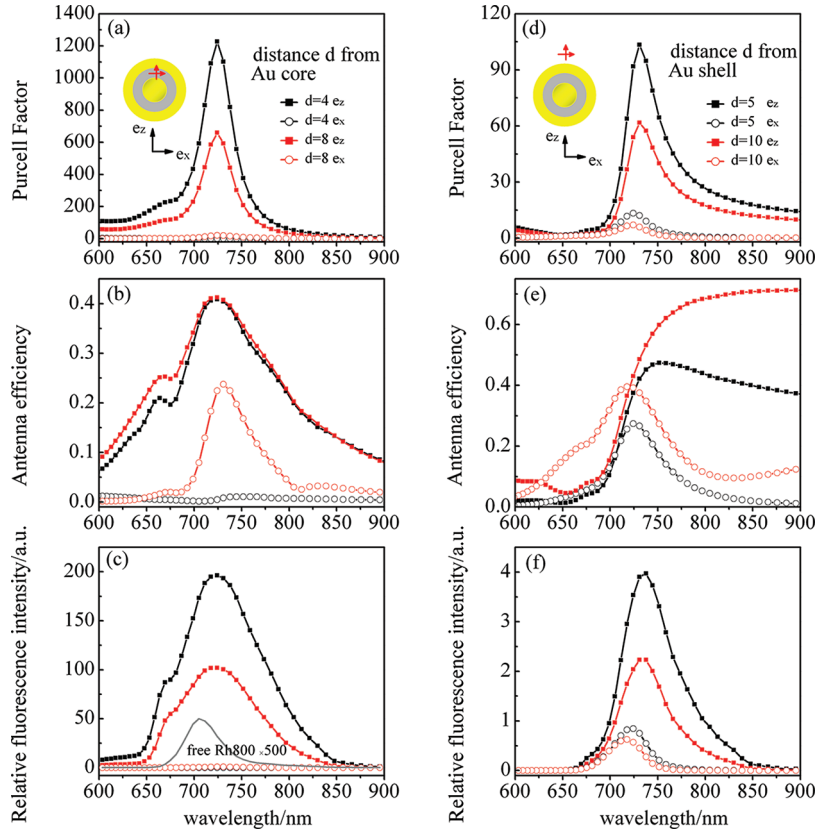

Figure 6. The Purcell factor, the antenna efficiency of the nanoshell, and the relative fluorescence intensity of an emitter placed inside (left) and outside (right) the "MNS-18-30-12". The footnote square and circle represent the orientation of the dipole with e_z and e_x orientation. The separation between the emitter and the gold core is fixed at 4 and 8 nm for emitter inside. The separation between the emitter and the nanoshell surface is fixed at 5 and 10 nm for emitter outside.

In consideration of experiments feasibility, a gold nanosphere concentrically placed in a gold nanoshell is calculated and optimized as a promising MNS structure. Indeed, such a MNS has already been experimentally synthesized with silica filling the cavity: its plasmon resonance wavelength λ_{max} changes almost in the same way as does NS under size modifications. However, a new plasmon resonance peak appears due to some plasmon hybridization between the core and the shell.[56] For a fixed MNS size, increasing the Au core radius results in a red-shift of the plasmon resonance as the coupling between the core and the shell becomes stronger (see the Supporting Information). So, several differently sized MNSs were chosen to present dipolar plasmon resonances in exact correspondence with the emission maximum of Rh800 (λ: 705 nm). For simplicity of notations, a MNS characterized by an 18 nm gold core radius, a 12 nm-thick middle dielectric layer, and a 12 nm-thick external shell layer is simply named "MNS-18-30-12". Dipolar emitters are placed within the silica middle layer at the same separation (4 nm) from the Au core surface regardless of the size of the MNSs studied. Typical fluorescence intensities brought by this improved structure are shown in Figure 4. Similarly to NSs, the fluorescence enhancement results from a

dx.doi.org/10.1021/jp2125944 | J. Phys. Chem. C 2012, 116, 8804−8812

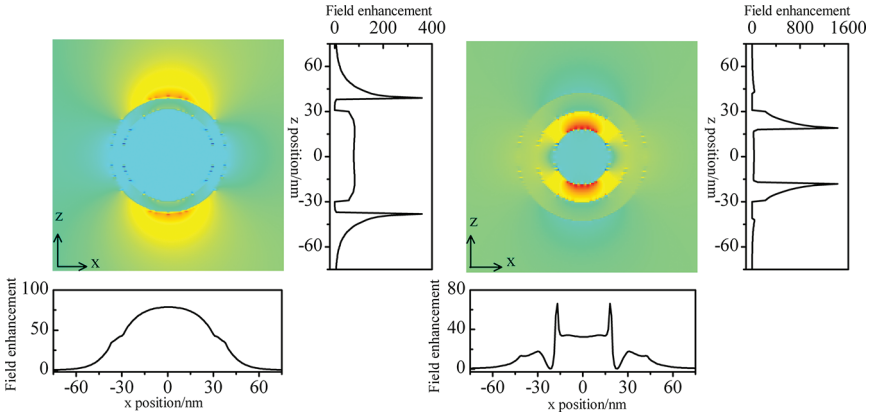

Figure 7. The field distribution and field enhancement at $x-z$ plane near the "NS-30-8" (a) and "MNS-18-30-12" (b) illuminated by the light propagating along the y direction at λ = 705 nm (resonance). Corresponding field enhancements as compared to the free space are plotted on the right along the $x-z$ cross-section, respectively.

competition between two main factors, that is, the radiative and nonradiative processes both included in the Purcell factor and the antenna efficiency. Figure 4 shows that the "MNS-18-30-12" leads to the best fluorescence enhancement. Interestingly, all MNS present significantly larger field enhancement than do NSs. For instance, the fluorescence enhancement is improved by about 1 order of magnitude as compared to the best NS "NS-30-8". It is should be noted that "MNS-26-40-25" also gives a satisfying fluorescence enhancement and may be even better if the particle encapsulated a lot of molecules in the middle layer (the cavity volume of this latter being greater than that of MNS-18-30-12 and then would lead to a smaller concentration quenching).

To characterize completely the MNS as a fluorescence enhancer, the effects of the emitter's position and orientation have also to be investigated and compared to those observed in the NSs above. First, the fluorescence enhancement as a function of the MNS−emitter separation is plotted in Figure 5. Again, the MNS fluorescence enhancement is distance and wavelength dependent, and it is desirable that the plasmon resonance of MNS overlaps both the excitation and the emission bands of the fluorophore to reach a maximal enhancement. For molecules encapsulated within the silica layer, the closer to the core surface, the greater the optical field is enhanced, and the more important the fluorescence enhancement becomes. The fluorescence enhancement decreases with the distance to the gold core, and for very short separation (precisely until 3 nm, a size characteristic of the Förster distance) between the emitter and both metal surfaces, there is still an unexpected high fluorescence enhancement without obvious quenching (Figure 5a). MNSs then significantly improve the fluorescence enhancement in almost the entire intermetallic volume, reducing at the same time the probability of fluorescence quenching. The performing features of such MNSs certainly originate from their unique plasmonic properties that allow an improved field enhancement without decreasing the Purcell factor or reducing the antenna efficiency. A usually sphere particle presents much less fluorescence enhancement effect and displays fluorescence quenching obviously when the emitter−particle separation is below 3 nm.[46−48] While the fluorescence intensity is enhanced near the spherical core of the MNSs greatly and shows no obvious quenching effect, even the separation between the molecule and the gold core is very small. The MNS's gold shell and plasmonic coupling effect are believed to modify the molecular fluorescence behaviors differently from the single spherical nanoparticle (see Figure 5c and the Supporting Information). A plausible explanation is small dissipation in the near-infrared region of gold material where the imaginary part of the dielectric function is smaller than that in the visible range.

The strong coupling between the adjacent gold core and gold shell leads to the incident electromagnetic field being squeezed into the gap. Hence, the silica layer can be called as "hot volume" optimal for fluorescence enhancement. In contrast to the NS, the enhancement is mainly confined locally within the silica layer, and the plasmonic-enhanced effect is negligible outside the MNSs. This should certainly be attributed to a strong coupling effect between the metallic core and shell so that such Matryoshka-nanoshells appear to be brighter fluorescence probes by encapsulating fluorophores within the MNS's middle layer. Such anisotropic behavior can be further verified by 3D calculations. As can be seen in Figure 6, MNS enhanced fluorescence is dependent on dipole orientation and excitation light polarization. Both inside and outside the dielectric region of the MNS, there is strong dependence on the emitter orientation. As expected, an increased enhancement, corresponding to a most effective coupling between the emitter and the MNS, is observed when light polarization and dipole orientation coincide. This is inherent to the near-field interactions between the nanostructure and the incident optical field as well as interactions between the MNS antenna and the fluorophores.

Field Distribution around the Nanoshell and Matryoshka-Nanoshell. To gain more insight into the plasmonic-enhanced fluorescence and to obtain better structural optimization, we visualize the field distribution around the nanostructures. The 3D-FDTD is employed to calculate the electric field under illumination of light propagating along the x direction and polarized according to the z direction with a wavelength λ corresponding to surface plasmon resonance bands. Figure 7 shows both the field distribution and the field enhancement in the $x-z$ section around the center of the nanoconstruct. For the nanoshell "NS-30-8", field enhancements are observed both inside and outside. Higher enhancement occurs along the polarization direction of the incident light in the vicinity of the outside region, and the field decays exponentially with the distance increasing from the shell surface, while within the core region no polarization depend-

dx.doi.org/10.1021/jp2125944 | J. Phys. Chem. C 2012, 116, 8804−8812

ence is observed. The optical field distribution within the core region is much more homogeneous as compared to the external area of the NS. For the MNS, the "hot volume" (i.e., the gap between the gold core and the shell) concentrates the greater part of the optical field enhancement effect, and the MNS construct presents extremely strong field enhancement with the gap. As the structure compresses and traps the optical field into the narrow space of the silica layer, the field distribution is no longer uniform inside the MNS. It can be also seen that the maximal enhancement of the field is found along the polarization direction of the incident light, whereas it exhibits an asymmetric distribution at the vicinity of the outside surface. Nevertheless, the MNS structure generally produces stronger field enhancements than does NS. When taking into account that the fluorescence enhancement depends not only on the strong local field intensity but also on the quantum efficiency of the molecule in the presence of the metallic structure, the MNSs obtained by a rational design are found to present all of the advantages shown above. Indeed, the Purcell factor and the field enhancement are greatly improved while the relative high quantum efficiency is maintained at the same time. Furthermore, the encapsulated fluorophores within the MNS can be prevented from photobleaching because of the gold shell that could hinder the entrance of oxygen. Also, the encapsulated fluorophore would become more stable because the coupling between the emitter and the metallic structure would result in a shorter lifetime, which would decrease the fluorophore damage because of a shorter stay in excitation state. All of these factors indicate MNSs as a promising probe for enhancing molecular fluorescence for biological imaging applications or an idea platform of surface plasmon amplification by the stimulated emission of radiation based on fluorescent plasmonic nanostructures.[57]

CONCLUSIONS

We designed and optimized the nanostructure of single NS (silica core/gold) shell and MNS (gold core/silica layer/gold shell) as fluorescence probes by FDTD calculation. Our results reveal that overlapping the plasmon band with the excitation and emission spectra of the emitter is desirable for obtaining a maximal fluorescence enhancement. By adjusting the relative dimensions of the composite structures, high fluorescence enhancements were successfully achieved. For the optimized single gold NS, fluorescent emitters embedded inside can experience substantial fluorescence enhancement without strict requirements upon the position and dipole orientations, while fluorescent emitters placed outside the NS can reach higher fluorescence intensity near the surface when their orientations coincide with that of the light polarization. Additionally, we propose a MNS construct consisting of a gold core placed concentrically in a gold nanoshell as an efficient fluorescent probe with a compact geometry and an extremely high local fluorescence enhancement within the middle gap layer. At the same time, the emitter orientation and the incident light polarization dependence of the fluorescence enhanced by MNS were investigated and found to be different from those found for NSs. The results presented here provide a new class of fluorescent probes with significant fluorescence intensity that show great promises for fluorescence detection with high sensitivity required, for instance, by biological imaging applications.

ASSOCIATED CONTENT

Supporting Information

Gold nanoshells' plasmon resonance maximum for different core size and shell thickness, and fluorescence enhancement for gold spherical nanoparticles as a function of particle−molecule separation. This material is available free of charge via the Internet at http://pubs.acs.org.

AUTHOR INFORMATION

Corresponding Author

*E-mail: guowei.lu@pku.edu.cn (G.L.); qhgong@pku.edu.cn (Q.G.).

Notes

The authors declare no competing financial interest.

ACKNOWLEDGMENTS

This work was supported by the National Basic Research Program of China (grant nos. 2007CB307001 and 2009CB930504) and the National Natural Science Foundation of China (grant nos. 61008026, 11121091, 90921008).

REFERENCES

(1) Frangioni, J. V. *Curr. Opin. Chem. Biol.* **2003**, *7*, 626−634.
(2) Waggoner, A. *Curr. Opin. Chem. Biol.* **2006**, *7*, 62−66.
(3) Oliver, T.; Helge, E.; Martin, H.; Laurent, G.; Renato, F.; Gregory, G.; Christel, P.; Philippe, L.; Brahim, L.; Laurent, C.; Daniel, C. *Chem. Rev.* **2008**, *108*, 1565−1587.
(4) Licha, K. *Top. Curr. Chem.* **2002**, *222*, 1−29.
(5) Bruchez, M.; Moronne, M.; Gin, P.; Weiss, S.; Alivisatos, A. P. *Science* **1998**, *281*, 2013−2016.
(6) Parvesh, S.; Scott, B.; Glenn, W.; Swadeshmukul, S.; Brij, M. *Adv. Colloid Interface Sci.* **2006**, *123*, 471−485.
(7) Ow, H.; Larson, D. R.; Srivastava, M.; Baird, B. A.; Webb, W. W.; Wiesner, U. *Nano Lett.* **2005**, *5*, 113−117.
(8) Yang, S.; Wang, X.; Wang, H.; Lu, F.; Luo, P.; Cao, L.; Meziani, M. J.; Liu, J.; Liu, Y.; Chen, M.; et al. *J. Phys. Chem. C* **2009**, *113*, 8110−18114.
(9) Huang, B.; Wang, W.; Bates, M.; Zhuang, X. *Science* **2008**, *319*, 810−813.
(10) Mikhail, Y. B.; Samuel, A. *Chem. Rev.* **2010**, *110*, 2641−2684.
(11) Oldenburg, S. J.; Averitt, R. D.; Westcott, S. L.; Halas, N. J. *Chem. Phys. Lett.* **1998**, *288*, 243−247.
(12) Hirsch, L. R.; Gobin, A. M.; Lowery, A. R.; Tam, F.; Drezek, R. A.; Halas, N. J.; West, J. L. *Annu. Biomed. Eng.* **2006**, *24*, 15−22.
(13) Lai, S.; Grady, N. K.; Kundu, J.; Levin, C. S.; Lassiter, J. B.; Halas, N. J. *Chem. Soc. Rev.* **2008**, *37*, 898−911.
(14) West, J. L.; Halas, N. J. *Annu. Rev. Biomed. Eng.* **2003**, *5*, 285−292.
(15) Hirsch, L. R.; Jackson, J. B.; Lee, A.; Halas, N. J.; West, J. *Anal. Chem.* **2003**, *75*, 2377−2381.
(16) Zhang, J.; Fu, Y.; Mei, Y.; Jiang, F.; Lakowicz, J. R. *Anal. Chem.* **2010**, *82*, 4464−4471.
(17) Loo, C.; Lowery, A.; Halas, N. J.; West, J.; Dreaek, R. *Nano Lett.* **2005**, *5*, 709−711.
(18) Tam, F.; Goodrich, G. P.; Johnson, B. R.; Halas, N. J. *Nano Lett.* **2007**, *7*, 496−501.
(19) Bardhan, R.; Grady, N. K.; Halas, N. J. *Small* **2008**, *4*, 1716−1722.
(20) Zhang, J.; Gryczynski, I.; Gryczynski, Z.; Lakowicz, J. R. *J. Phys. Chem. B* **2006**, *110*, 8986−8991.
(21) Zhang, J.; Fu, Y.; Lakowicz, J. R. *J. Phys. Chem. C* **2007**, *111*, 1955−1961.
(22) Zhang, J.; Fu, Y.; Lakowicz, J. R. *J. Phys. Chem. C* **2009**, *113*, 19404−19410.
(23) Zhang, J.; Fu, Y.; Lakowicz, J. R. *J. Phys. Chem. C* **2011**, *115*, 7255−7260.

(24) Jin, Y.; Gao, X. *Nat. Nanotechnol.* **2009**, *4*, 571−576.
(25) Zaiba, S.; Lerouge, F.; Gabudean, A.-M.; Focsan, M.; Lerme, J.; Gallavardin, T.; Maury, O.; Andraud, C.; Parola, S.; Baldeck, P. L. *Nano Lett.* **2011**, *11*, 2043−2047.
(26) Enderlein, J. *Appl. Phys. Lett.* **2002**, *80*, 315−317.
(27) Enderlein, J. *Phys. Chem. Chem. Phys.* **2002**, *4*, 2780−2786.
(28) Miao, X.; Brener, I.; Luk, T. S. *J. Opt. Soc. Am. B* **2010**, *27*, 1561−1570.
(29) Liaw, J.; Chen, J.; Chen, C.; Kuo, M. *Opt. Express* **2009**, *17*, 13532−13540.
(30) Kodali, A. K.; Llora, X.; Bhargava, R. *Proc. Natl. Acad. Sci. U.S.A.* **2010**, *107*, 13620−13625.
(31) Prodan, E.; Radloff, C.; Halas, N. J.; Nordlander, P. *Science* **2003**, *412*, 419−422.
(32) Taflove, A.; Hagness, S. C. *Computational Electrodynamics: The Finite-Difference Time-Domain Method*, 3rd ed.; Artech House: Norwood, MA, 2005.
(33) Oskooi, A. F.; Roundy, D.; Ibanescu, M.; Bermel, P.; Joannopoulos, J. D.; Johnson, S. G. *Comput. Phys. Commun.* **2010**, *181*, 687−702.
(34) Kaminski, F.; Sandoghdar, V.; Agio, M. *J. Comput. Theor. Nanosci.* **2007**, *4*, 635−643.
(35) Mohammadi, A.; Sandoghdar, V.; Agio, M. *New J. Phys.* **2008**, *10*, 105015−105028.
(36) Mohammadi, A.; Kaminski, F.; Sandoghdar, V.; Agio, M. *J. Phys. Chem. C* **2010**, *114*, 7372−7377.
(37) Johnson, P. B.; Christy, R. W. *Phys. Rev. B* **1972**, *6*, 4370−4379.
(38) Lal, S.; Link, S.; Halas, N. J. *Nat. Photonics* **2007**, *1*, 641−648.
(39) Jain, P. K.; El-Sayed, M. A. *Nano Lett.* **2007**, *7*, 2854−2858.
(40) Abugo, O. O.; Nair, R.; Lakowicz, J. R. *Anal. Chem.* **2000**, *279*, 142−150.
(41) Jin, T. *Sensors* **2010**, *10*, 2438−2449.
(42) Sanchez-Valencia, J. R.; Aparicio, F. J.; Espinos, J. P.; Gonzalez-Elipe, A. R.; Barranco, A. *Phys. Chem. Chem. Phys.* **2011**, *13*, 7071−7082.
(43) Shimiza, K. T.; Woo, W. K.; Fisher, B. R.; Eisler, H. J.; Bawendi, M. G. *Phys. Rev. Lett.* **2002**, *89*, 117401−117404.
(44) Kuhn, S.; Hakansion, U.; Rogobete, L.; Sandoghdar, V. *Phys. Rev. Lett.* **2006**, *97*, 017402−017405.
(45) Trabesinger, W.; Kraner, A.; Kreiter, M.; Hecht, B.; Wild, U. P. *Appl. Phys. Lett.* **2002**, *81*, 2118−2120.
(46) Dubertret, B.; Calame, M.; Libchaber, A. J. *Nat. Biotechnol.* **2001**, *19*, 365−370.
(47) Lee, J.; Govorov, A. O.; Dulka, J.; Kotov, N. A. *Nano Lett.* **2004**, *4*, 2323−2330.
(48) Anger, P.; Bharadwaj, P.; Novotny, L. *Phys. Rev. Lett.* **2006**, *96*, 113002−113005.
(49) Rogobete, L.; Kaminski, F.; Agio, M.; Sandoghdar, V. *Opt. Lett.* **2007**, *32*, 1623−1625.
(50) Lu, G.; Zhang, T.; Li, W.; Hou, L.; Liu, J.; Gong, Q. *J. Phys. Chem. C* **2011**, *115*, 15822−15828.
(51) Hartling, T.; Reichenbach, P.; Eng, L. M. *Opt. Express* **2007**, *15*, 12806−12817.
(52) Martini, M.; Perriat, P.; Montagna, M.; Pansu, R.; Julien, C.; Tillement, O.; Roux, S. *J. Phys. Chem. C* **2009**, *113*, 17669−17677.
(53) Talley, C. E.; Jackson, J. B.; Oubre, C.; Grady, N. K.; Hollars, C. W.; Lane, S. M.; Huser, T. R.; Nordlander, P.; Halas, N. J. *Nano Lett.* **2005**, *5*, 1569−1574.
(54) Xu, H. *Phys. Rev. B* **2005**, *72*, 073405.
(55) Mukherjee, S.; Sobhani, H.; Lassiter, J. B.; Bardhan, R.; Nordlander, P.; Halas, N. J. *Nano Lett.* **2010**, *10*, 2694−2701.
(56) Bardhan, R.; Mukherjee, S.; Mirin, N. A.; Levit, S. D.; Nordlander, P.; Halas, N. J. *J. Phys. Chem. C* **2010**, *114*, 7378−7383.
(57) Noginov, M. A.; Zhu, G.; Belgrave, A. M.; Bakker, R.; Shalaev, V. M.; Narimanov, E. E.; Stout, S.; Herz, E.; Suteewong, T.; Wiesner, U. *Nature* **2009**, *460*, 1110−1113.